

A Novel ANSMC Algorithm for Tracking Control of 3-DOF Planar Parallel Manipulators

Thanh Nguyen Truong, Anh Tuan Vo, and Hee-Jun Kang*

Department of Electrical, Electronic and Computer Engineering, University of Ulsan, Ulsan 44610, South Korea

Email: thanhnguyen151095@gmail.com, voanhtuan2204@gmail.com

*Correspondence: hjkang@ulsan.ac.kr

Abstract—Our article mainly focuses on dealing with several limitations of conventional sliding mode control (SMC), proportional-integral-derivative SMC (PID-SMC), and integral SMC (ISM) for 3-DOF robotic manipulators at the same time. The paper focuses on three main points: improving the control accuracy, reducing chattering phenomena, and the convergence speed of the system states. Therefore, we develop a novel adaptive neural sliding mode control (ANSMC) algorithm for 3-DOF parallel robotic manipulators which has a complicated dynamic model, including modeling uncertainties, frictional uncertainties, and external disturbances. The control method is designed from three main control techniques, including ISMC, Radial Basis Function Neural Network (RBFNN), and the adaptive technique. First, a new integral terminal sliding mode (ITSM) surface is proposed to enhance the response rate and convergence rate. Second, RBFNN is employed to address disturbances and uncertainties. Besides, RBFNN also plays the role in reducing chattering behavior. While the adaptive technique is integrated into the reaching control law to remove the need for the upper bound values. Consequently, the proposed control system provides a high tracking accuracy and fast convergence rate. The chattering phenomena are significantly diminished in control signals. Simulation results on a 3-DOF parallel manipulator have confirmed the effectiveness of the proposed control method.

Keywords—adaptive controller, planar parallel manipulator, radial basis function neural network, sliding mode controller

I. INTRODUCTION

Parallel robot manipulators have great benefits including high operation speed with good accuracy, less affected by gravity during motion, and a high rigidity that may be obtained with a small mass of the manipulator. Therefore, their applications have appeared in many fields. For example, flight simulators, automobile simulators, assembly of PCBs, high-speed/high-precision milling machines, and so on. Accompanying flexibility in operation is the complexity of the dynamic model and several drawbacks such as kinematic complication, singularity problems, or workspace limitation due to their closed-loop structure. Therefore, the operation performance expectations from parallel robot

manipulators should be started from the advanced control methods.

Sliding Mode Control (SMC) is a robust control methodology for handling the approximation model which exists the unknown functions or uncertain terms [1]–[8]. To obtain the desired control performance for the system with the presence of uncertainties and external disturbances, the common way is to increase switching gain in the reaching control law. Particularly, the value of the switching gain is selected as a value bigger than the uncertainty upper bound value. This technique increases the robustness and the stability of the control input but that also adds chattering phenomena. Unfortunately, the upper boundaries of the uncertain components are the unknown values, which are not available in actual applications. Moreover, the trajectories of the system states under the conventional SMC will slowly respond and slowly converge to the sliding surface when it uses a not large switching gain value. In the literature, to deal with the mentioned problem in SMC, various control methods based on other methods such as PID-SMC [9], [10], ISMC [11], [12] have been suggested to enhance convergence and response. In general, these methods have faster response and convergence compared to conventional SMCs. However, the main shortcomings of SMC have yet to be addressed such as chattering, the upper boundaries of the uncertain components, and the exact computation of the dynamic model. According to the knowledge of the authors, all three weaknesses can be solved simultaneously by using neural networks (NNs) [13]–[18]. The NNs can approximate unknown functions, functions are very difficult to linearize exactly (e.g. dynamic model, unknown uncertainty, or external disturbance). Because NN has arbitrarily approximated unknown functions. This entails only determining the upper bound value of the approximate error from the NN. This upper limit value is normally small and easily predictable. Accordingly, the value of the reaching control law is also used as a small value. As a result, chattering behavior is also lesser likely to appear in control inputs. Considering aspects such as simple design, strong approximation, convergence speed, and applicability in existing real systems, the radial basis function neural network (RBFNN) has the mentioned features [19].

From the stated reason, our article mainly focuses on dealing with several limitations of conventional SMC, PID SMC, and ISMC at the same time. The paper focuses on three main points: improving the control accuracy, reducing chattering phenomena, and the convergence speed of the system states. Therefore, we develop a novel trajectory tracking control algorithm for 3-DOF parallel robotic manipulators by introducing a new completely ITSM surface. The control method is designed from three main techniques, including ISMC, RBFNN, and the adaptive technique. First, a new ITSM sliding mode surface is proposed to improve the response rate and convergence rate. Second, RBFNN is employed to address disturbances and uncertainties, while the adaptive technique is integrated into the reaching control law to remove the need for the upper bound values. Consequently, the proposed control system provides a higher tracking accuracy and faster convergence rate than the classic SMC and another method [20]. In addition, the chattering is significantly diminished in control signals and the requirement of upper boundary value for sliding gain is also eliminated by using the adaptive technique like in [20].

Our paper is arranged as follows. The first section is an introduction. Section II describes the kinematic and dynamic model of 3-DOF planar parallel manipulators. Section III reports the classic SMC and the control proposal. Simulations are conducted in section IV. Finally, conclusions are given in section V.

II. THE 3-DOF PLANAR PARALLEL MANIPULATORS

A. The Geometry of the 3-DOF Planar Parallel Manipulators

The geometry of the 3-DOF planar parallel robotic manipulators is described in Fig. 1. It operates on a horizontal plane in an Oxy reference frame. There are three active joints, six passive joints, and the end-effector of this manipulator. Its link lengths are $l_1 = A_i B_i$, $l_2 = B_i C_i$, ($i = 1, 2, 3$), and the end-effector $C_1 C_2 C_3$ is an equilateral triangle in which $l_3 = C_i P$ is a radius of the circle encircling the three vertex points. In Fig. 1, $\theta_a = [\theta_{a1}, \theta_{a2}, \theta_{a3}]^T$ denotes the vector of three active joint angles, $\theta_p = [\theta_{p1}, \theta_{p2}, \theta_{p3}]^T$ denotes the vector of three passive joint angles, and $P = [x_p, y_p, \phi_p]^T$ denotes the vector of the end-effector position.

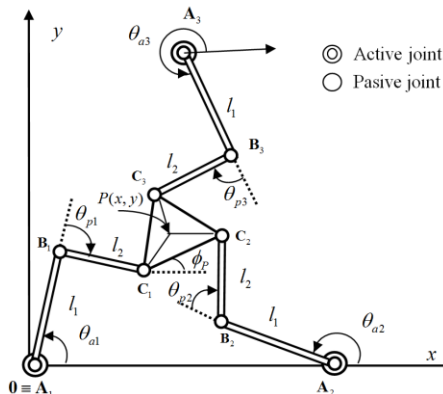


Figure 1. The kinematics of 3-DOF planar parallel manipulators.

B. Dynamic Models of 3 DOF Planar Parallel Manipulators

The dynamic model for a 3-DOF parallel robotic manipulator is given as in reference [17]:

$$M\ddot{\theta}_a + C\dot{\theta}_a + F_a + \varrho(t) = \tau_a \quad (1)$$

where $\dot{\theta}_a = [\dot{\theta}_{a1} \ \dot{\theta}_{a2} \ \dot{\theta}_{a3}]^T$ and $\ddot{\theta}_a = [\ddot{\theta}_{a1} \ \ddot{\theta}_{a2} \ \ddot{\theta}_{a3}]^T$ are respectively the angular velocity vector and angular acceleration vector at each active joint. $M = \hat{M} + \Delta M \in \mathbb{R}^{3 \times 3}$ is the real inertia matrix. $C = \hat{C} + \Delta C \in \mathbb{R}^{3 \times 3}$ denotes the real Coriolis and centrifugal force matrix. $\hat{M} \in \mathbb{R}^{3 \times 3}$ and $\hat{C} \in \mathbb{R}^{3 \times 3}$ are the estimated matrices of M and C , respectively. $F_a \in \mathbb{R}^{3 \times 1}$ and $\varrho(t) \in \mathbb{R}^{3 \times 1}$ are the friction force vector and disturbance vector at the active joints, respectively. $\Delta M \in \mathbb{R}^{3 \times 3}$ and $\Delta C \in \mathbb{R}^{3 \times 3}$ are the bounded modeling errors. Reference [17] contains a detailed description of M and C .

The whole external disturbances and uncertainties are defined as:

$$\Delta\tau_a = \Delta M_a \ddot{\theta}_a + \Delta C_a \dot{\theta}_a + F_a + \varrho(t) \quad (2)$$

Based on (1) and (2), the dynamic model is rewritten as:

$$\hat{M}\ddot{\theta}_a + \hat{C}\dot{\theta}_a + \Delta\tau_a = \tau_a \quad (3)$$

Assumption 1: [21] Suppose that the whole external disturbances and unknown uncertainties are bounded by:

$$|\Delta\tau_a| \leq \theta \quad (4)$$

where θ is a positive constant.

III. THE PROPOSED CONTROLLER

A. Classic Sliding Mode Control

The position error and the velocity error are defined as follows:

$$\begin{cases} e = \theta_d - \theta_a \in \mathbb{R}^{3 \times 1} \\ \dot{e} = \dot{\theta}_d - \dot{\theta}_a \in \mathbb{R}^{3 \times 1} \end{cases} \quad (5)$$

where $\theta_d \in \mathbb{R}^{3 \times 1}$ stands for the desired path of the active joint angles, $\theta_a \in \mathbb{R}^{3 \times 1}$ is the real path of the active joint angles.

A linear sliding surface is selected as in [2] for the 3-DOF planar parallel manipulator:

$$s = \dot{e} + ce \in \mathbb{R}^{3 \times 1} \quad (6)$$

where $c = \text{diag}(c_1, c_2, c_3) \in \mathbb{R}^{3 \times 3}$ is a positive matrix.

For the desired performance of the robot system, the SMC is designed as:

$$\begin{cases} \tau_a = \tau_{eq} + \tau_r \\ \tau_{eq} = \hat{M}(\ddot{\theta}_d + c\dot{e}) + \hat{C}(\theta_a, \dot{\theta}_a)(\dot{\theta}_d + ce) \\ \tau_r = \kappa \text{sign}(s) + Hs \end{cases} \quad (7)$$

where $\kappa = \text{diag}(\kappa_1, \kappa_2, \kappa_3)$, and $H = \text{diag}(H_1, H_2, H_3)$ are positive diagonal matrices. The term of $\tau_{eq} \in \mathbb{R}^{3 \times 1}$ is the equivalent control that maintains the system states on the sliding surface, while the term of $\tau_r \in \mathbb{R}^{3 \times 1}$

manipulates the system states from initial values to reach the sliding surface. In addition, τ_r also plays the role in coping with the influence of uncertain nonlinear terms. To achieve the asymptotic stability of the control system, the sliding gain κ must be selected greater than the upper boundary value of the lumped uncertain terms θ . That generates two problems, including the existence of the chattering phenomena and the requirement of the mentioned upper boundary value. To solve two problems at once, RBFNN is employed to address disturbances and uncertainties, while the adaptive technique is integrated into the reaching control law to remove the need for the upper bound values. Furthermore, the convergence rate of the classic SMC also needs to be improved to provide better control performance for parallel robotic manipulators. That also will be handled in the next subsection.

B. Novel Adaptive Neural Network Sliding Mode Controller

Considering the dynamic model of the robot (3), a PID sliding surface is designed as in [22], which offers a faster response and lesser steady-state error than the traditional sliding surface:

$$s = \dot{e} + ce + \beta \int edt \quad (8)$$

where $s = [s_1 \ s_2 \ s_3]^T \in \mathbb{R}^{3 \times 1}$, $c = \text{diag}(c_1, c_2, c_3) \in \mathbb{R}^{3 \times 3}$ and $\beta = \text{diag}(\beta_1, \beta_2, \beta_3) \in \mathbb{R}^{3 \times 3}$ are positive matrices.

A novel ITSM surface is designed to improve sliding surface (8) as follows:

$$s_i = \dot{e}_i + c_i |e_i|^{m_i} \text{sgn}(e_i) + \beta_i \int |e_i|^{n_i} \text{sgn}(e_i) dt \quad (9)$$

$, i = 1, 2, 3$

where $c_i, \beta_i > 0$, $m_i = 0.5(p + q) + 0.5(p - q) \text{sgn}(|e_i| - 1)$, $n_i = 0.5(l + r) + 0.5(l - r) \text{sgn}(|e_i| - 1)$, $p > 1$, $l > 1$, $0 < q, r < 1$, $s = [s_1 \ s_2 \ s_3]^T \in \mathbb{R}^{3 \times 1}$.

Remark 1. Once $|e_i|$ is much greater than 1, $m_i = p > 1$ and $n_i = l > 1$. $|-c_i |e_i|^{m_i} \text{sgn}(e_i)|$ and $|\beta_i \int |e_i|^{n_i} \text{sgn}(e_i) dt|$ play the role that offers faster convergence than (8). It infers that the error trajectories in (9) will quickly converge to 1 from any initial conditions. Once $|e_i|$ is smaller than 1, $m_i = q < 1$ and $n_i = r < 1$. $|-c_i |e_i|^{m_i} \text{sgn}(e_i)|$ and $|\beta_i \int |e_i|^{n_i} \text{sgn}(e_i) dt|$ determine finite-time convergence and convergence speed of the proposed sliding surface is also faster than those (8) in this phase. It is concluded that the novel proposed sliding surface has been improved significantly compared to (8).

From (9), we can get:

$$\dot{\theta}_{ai} = \dot{\theta}_{di} + c_i |e_i|^{m_i} \text{sgn}(e_i) + \beta_i \int |e_i|^{n_i} \text{sgn}(e_i) dt - s_i \quad (10)$$

Let $A_i = \dot{\theta}_{di} + c_i |e_i|^{m_i} \text{sgn}(e_i) + \beta_i \int |e_i|^{n_i} \text{sgn}(e_i) dt$, $i = 1, 2, 3$, $A = [A_1 \ A_2 \ A_3]^T$. Therefore, (10) in matrix form as follows:

$$\dot{\theta}_a = A - s \quad (11)$$

Differentiating s in (9) to time, we have:

$$\dot{s}_i = \ddot{e}_i + m_i c_i |e_i|^{m_i-1} \dot{e}_i + \beta_i |e_i|^{n_i} \text{sgn}(e_i) \quad (12)$$

$, i = 1, 2, 3$

To simplify, let $B_i = m_i c_i |e_i|^{m_i-1} \dot{e}_i + \beta_i |e_i|^{n_i} \text{sgn}(e_i)$, $i = 1, 2, 3$, $B = [B_1 \ B_2 \ B_3]^T$. Equation (12) is presented in vector form as:

$$\dot{s} = \ddot{e} + B = \ddot{\theta}_d - \ddot{\theta}_a + B \quad (13)$$

Multiplying both sides of (13) with \hat{M} , we have

$$\begin{aligned} \hat{M}\dot{s} &= \hat{M}(\ddot{\theta}_d + B) - \hat{M}\ddot{\theta}_a \\ &= \hat{M}(\ddot{\theta}_d + B) - (\tau_a - \hat{C}\dot{\theta}_a - \Delta\tau_a) \\ &= \hat{M}(\ddot{\theta}_d + B) + \hat{C}(A - s) + f - \tau_a \end{aligned} \quad (14)$$

where $f = \Delta\tau_a \in \mathbb{R}^{3 \times 1}$.

In fact, the term f is an unknown component. To simplify control design and improve control performance, this term should be approximated to provide the closed-loop control system. In this paper, the term f is estimated precisely by using an RBFNN.

The structure of RBFNN is depicted in Fig. 2. It consists of three layers: an input layer, a hidden layer with a non-linear RBF activation, and a linear output layer.

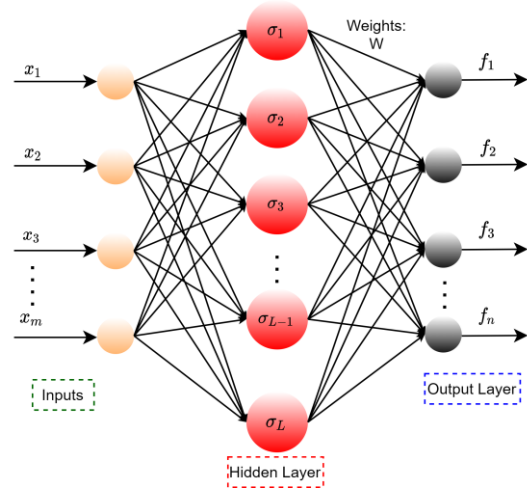


Figure 2. The structure of RBFNN.

The algorithm of an RBFNN is expressed as follows:

$$\begin{aligned} \sigma_j &= \exp\left(-\frac{\|x - z_j\|^2}{y_j^2}\right), j = 1, 2, \dots, L \\ f &= W^T \sigma(x) + \zeta \end{aligned} \quad (15)$$

where x is the input state of the NN, m is the input number of the NN, L is the number of hidden layer nodes in the NN, n is the output number of the NN, z_j and y_j are the center and width of the hidden neuron j , and $\|\cdot\|$ denotes the Euclidean norm. $\sigma(x) = [\sigma_1 \ \sigma_2 \ \dots \ \sigma_L]^T$ is the output of the Gaussian function, $W \in \mathbb{R}^{L \times n}$ is NN weight, $\zeta \in \mathbb{R}^{n \times 1}$ is the approximation error of NN, and $|\zeta| \leq \zeta_N$.

The input of RBFNN is chosen as:

$$x = [e^T \ \dot{e}^T]^T \in \mathbb{R}^{6 \times 1} \quad (16)$$

The output of RBFNN is given as follows:

$$\hat{f}(x) = \hat{W}^T \sigma(x) \in \mathbb{R}^{3 \times 1} \quad (17)$$

The proposed controller is proposed as:

$$\begin{cases} \tau_a = \tau_{eq} + \hat{f}(x) + \tau_r \\ \tau_{eq} = \hat{M}(\ddot{\theta}_d + B) + \hat{C}A \\ \tau_r = \text{diag}(\hat{K}) \text{sgn}(s) + Hs \end{cases} \quad (18)$$

where $\hat{f}(x)$ is the output of RBFNN, which is used to approximate the whole uncertainties and external disturbances, $H = \text{diag}(H_1, H_2, H_3)$ is a positive matrix, $\hat{K} = [\hat{K}_1 \ \hat{K}_2 \ \hat{K}_3]^T$ is the adaptive vector, which is used to estimate the boundary values of the approximation errors of NN. The updating law of \hat{K} is expressed as:

$$\dot{\hat{K}}_i = \begin{cases} \gamma_i |s_i| & |s_i| > \lambda_i \\ 0 & |s_i| \leq \lambda_i \end{cases}, i = 1, 2, 3 \quad (19)$$

in which, $\gamma = \text{diag}(\gamma_1, \gamma_2, \gamma_3)$, γ_i and λ_i are positive constants.

The adaptation tuning law for the RBFNN is selected as

$$\dot{\hat{W}} = \Phi \sigma(x) s^T \quad (20)$$

where $\Phi = \text{diag}(\Phi_1, \Phi_2, \Phi_3)$ is a positive matrix.

The block diagram of the proposed control system is shown in Fig. 3.

To check the stability of the proposed control method, the following proof will be given as follows:

Proof.

The estimation errors of NN's weight and the boundary value of the NN's approximation error are respectively defined as:

$$\begin{aligned} \tilde{W} &= W - \hat{W} \in \mathbb{R}^{L \times 3} \\ \tilde{K} &= \zeta_N - \hat{K} \end{aligned}, \quad (21)$$

and the output estimation error is given as:

$$\begin{aligned} f - \hat{f}(x) &= W^T \sigma(x) + \zeta - \hat{W}^T \sigma(x) \\ &= \tilde{W}^T \sigma(x) + \zeta \end{aligned} \quad (22)$$

For stability investigation of the proposed controller, a positive definite Lyapunov function is selected as:

$$V = \frac{1}{2} s^T \hat{M} s + \frac{1}{2} \text{tr} \{ \tilde{W}^T \Phi^{-1} \tilde{W} \} + \frac{1}{2} \tilde{K}^T \gamma^{-1} \tilde{K} \quad (23)$$

Then, the time derivative of V is

$$\dot{V} = s^T \hat{M} \dot{s} + \frac{1}{2} s^T \dot{\hat{M}} s + \text{tr} \{ \tilde{W}^T \Phi^{-1} \dot{\tilde{W}} \} + \tilde{K}^T \gamma^{-1} \dot{\tilde{K}} \quad (24)$$

Applying the control input (18) to (14) and using (22), we have:

$$\begin{aligned} \hat{M} \dot{s} &= \hat{M}(\ddot{\theta}_d + B) + \hat{C}(A - s) + f \\ &\quad - (\hat{M}(\ddot{\theta}_d + B) + \hat{C}A + \hat{f}(x) + \tau_r) \\ &= -\hat{C}s + f - \hat{f}(x) - \tau_r \\ &= -\hat{C}s + \tilde{W}^T \sigma(x) + \zeta - \tau_r \end{aligned} \quad (25)$$

Substituting (18) and (25) into (24), one has

$$\begin{aligned} \dot{V} &= s^T (-\hat{C}s + \tilde{W}^T \sigma(x) + \zeta - \tau_r) + \frac{1}{2} s^T \dot{\hat{M}} s \\ &\quad - \text{tr} \{ \tilde{W}^T \Phi^{-1} \dot{\tilde{W}} \} - \tilde{K}^T \gamma^{-1} \dot{\tilde{K}} \\ &= 0.5 s^T (\dot{\hat{M}} - 2\hat{C}) s + \text{tr} \{ \tilde{W}^T (-\Phi^{-1} \dot{\tilde{W}} + \sigma(x) s^T) \} \\ &\quad + s^T (\zeta - \text{diag}(\hat{K}) \text{sgn}(s) - Hs) - \tilde{K}^T \gamma^{-1} \dot{\tilde{K}} \end{aligned} \quad (26)$$

By referring to the updating laws (19) and (20), (26) can gain:

$$\begin{aligned} \dot{V} &= 0.5 s^T (\dot{\hat{M}} - 2\hat{C}) s + s^T (\zeta - \text{diag}(\hat{K}) \text{sgn}(s) - Hs) \\ &\quad - (\zeta_N - \hat{K})^T |s| \\ &= 0.5 s^T (\dot{\hat{M}} - 2\hat{C}) s + (s^T \zeta - \zeta_N^T |s|) - s^T Hs \end{aligned} \quad (27)$$

From (27), it is known that the characteristic $s^T (\dot{\hat{M}} - 2\hat{C}) s = 0$ always exists in the robot. Thus, (27) becomes:

$$\begin{aligned} \dot{V} &= (s^T \zeta - \zeta_N^T |s|) - s^T Hs \\ &\leq \sum_{i=1}^3 (\zeta_i - \zeta_{Ni}) |s_i| - \sum_{i=1}^3 H_i s_i^2 \leq 0 \end{aligned} \quad (28)$$

We can see that $V \geq 0$ and $\dot{V} \leq 0$. Therefore, the proof is completed.

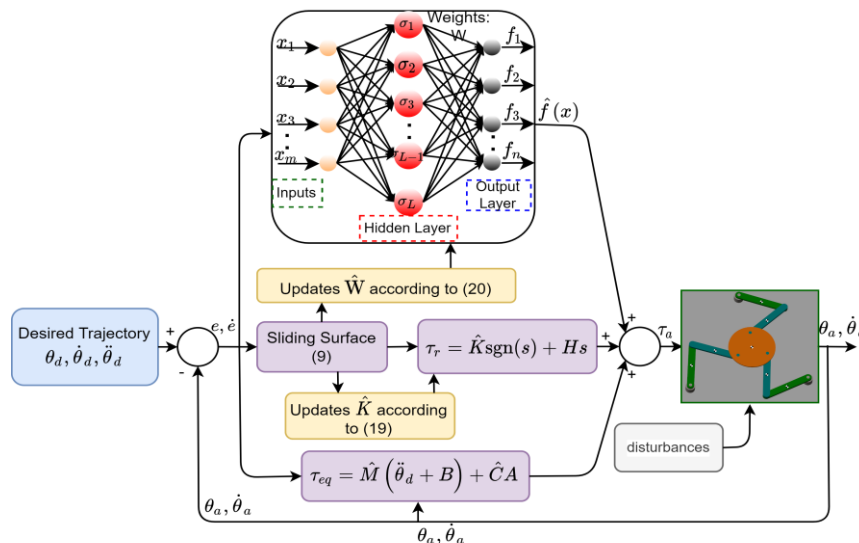


Figure 3. Block diagram of the proposed controller.

IV. SIMULATIONS AND RESULT

In this section, to demonstrate the effectiveness of the proposed control algorithm, a simulation is conducted for a 3-DOF planar parallel manipulator. This 3-DOF planar parallel manipulator was designed with SOLIDWORKS software (as shown in Fig. 4) and then embedded in a SIMULINK/MATLAB simulation environment using the Simscape Multibody Link toolbox. By using this method, the mechanical model in the simulation environment is almost identical to the real model. The designed parameters of this robotic manipulator are expressed in Table I. The configuration setting of the SIMULINK/MATLAB simulation environment is set under fixed-step with 0.001s fundamental sample time (ode5 Dormand-Prince). To verify the superior performance of the proposed controller and its improvement compared to two other methods including traditional SMC and method [20].

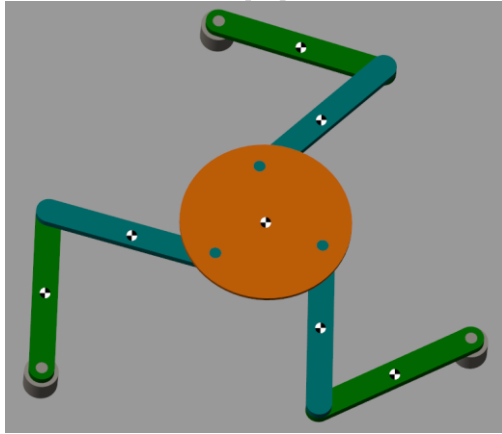


Figure 4. 3D SolidWorks model of a 3-DOF planar parallel manipulator.

TABLE I. THE DESIGN PARAMETERS OF THIS ROBOT SYSTEM

| Links | Length (m) | Center of mass (m) | Weight (kg) | Moment of inertia (kg.m ²) |
|--------------|---------------|--------------------|-------------|--|
| Active link | $l_1 = 0.2$ | 0.1 | 0.5028 | 1.9971×10^{-3} |
| Passive link | $l_2 = 0.2$ | 0.1 | 0.5512 | 2.4823×10^{-3} |
| End-effector | $l_3 = 0.072$ | 0 | 1.1985 | 6.0742×10^{-3} |

The control signal of traditional SMC is designed in (7).

The method [20] is constructed based on the combination of the PID sliding surface in (8), RBFNN, and the adaptive rule (19). The control signal of this method is given as follows:

$$\begin{cases} s = \dot{e} + ce + \beta \int edt \\ \tau_a = \tau_{eq} + \hat{f}(x) + \tau_r \\ \tau_{eq} = \hat{M}(\ddot{\theta}_d + c\dot{e} + \beta e) + \hat{C}(\dot{\theta}_d + ce + \beta \int edt) \\ \tau_r = \text{diag}(\hat{K}) \text{sgn}(s) + Hs \end{cases} \quad (29)$$

where $c = \text{diag}(c_1, c_2, c_3)$, $\beta = \text{diag}(\beta_1, \beta_2, \beta_3)$, and $H = \text{diag}(H_1, H_2, H_3)$ are positive matrices, $\hat{f}(x)$ is the output of RBFNN, \hat{K} is an adaptive vector that is updated by the rule (19).

The desired trajectory of the robot's end-effector is designed to track the following trajectory:

$$\begin{cases} x_d = 0.25 + 0.03 \cos(\pi t) \\ y_d = 0.5 \frac{\sqrt{3}}{6} + 0.03 \sin(\pi t) \\ \phi_{pd} = 0 \end{cases} \quad (30)$$

where x_d, y_d, ϕ_{pd} are desired trajectories.

The friction forces at active joints are modeled as follows:

$$F_a = \begin{bmatrix} 2\dot{\theta}_{a1} + 0.01 \text{sgn}(\dot{\theta}_{a1}) \\ 2\dot{\theta}_{a2} + 0.01 \text{sgn}(\dot{\theta}_{a2}) \\ 2\dot{\theta}_{a3} + 0.01 \text{sgn}(\dot{\theta}_{a3}) \end{bmatrix} \quad (31)$$

To test the robustness of control methods, the uncertain terms are assumed such as $\Delta M_a = 0.1M_a$, $\Delta C_a = 0.1C_a$, and the external disturbance is added to the control systems as follows:

$$q(t) = \begin{bmatrix} 0.4 \sin(2t) \\ 0.5 \sin(3t/2) \\ -0.4 \sin(t) \end{bmatrix}, \text{ at } t = 8s \quad (32)$$

The selected control parameters of the three control methods are chosen by repetitive testing to achieve the maximum performance of the three controllers. It is shown in Table II.

TABLE II. SELECTED CONTROL PARAMETERS OF THREE CONTROLLERS

| Control Methods | Control Parameters | Value |
|-----------------|--|---|
| SMC | c, κ, H | $\text{diag}(10,10,10), \text{diag}(0.9,0.9,0.9), \text{diag}(5,5,5)$ |
| Method [20] | c, β, H | $\text{diag}(10,10,10), \text{diag}(0.01,0.01,0.01), \text{diag}(5,5,5)$ |
| | $m, L, y_j, z, \Phi, W_0, \gamma_i, \lambda_i$ | $6, 7, 5, 0.5 \begin{bmatrix} -1.5; -1; -0.5; 0; 0.5; 1; 1.5 \\ \dots \\ -1.5; -1; -0.5; 0; 0.5; 1; 1.5 \end{bmatrix} \mathbb{R}^{6 \times 7}$ $\text{diag}(500,500,500), 0.1 \times I^{7 \times 3}$ 0.1, 2 |
| Proposed Method | $c_i, \beta_i, H, p, q, l, r$ | 10, 0.01, $\text{diag}(5,5,5)$ 1.6, 0.8, 1.6, 0.8 |
| | $m, L, y_j, z, \Phi, W_0, \gamma_i, \lambda_i$ | $6, 7, 5, 0.5 \begin{bmatrix} -1.5; -1; -0.5; 0; 0.5; 1; 1.5 \\ \dots \\ -1.5; -1; -0.5; 0; 0.5; 1; 1.5 \end{bmatrix} \mathbb{R}^{6 \times 7}$ $\text{diag}(500,500,500), 0.1 \times I^{7 \times 3}$ 0.1, 2 |

To analyze the position tracking accuracy and make an easy evaluation, tracking errors of active joints are considered after the period of convergence around the equilibrium point. The investigation time is $t = 1 \rightarrow 20s$, the control errors are calculated by (33) and the results are shown in Table III.

$$E_1 = \sqrt{\frac{1}{N} \sum_{i=1}^N (\theta_{1di} - \theta_{1ai})^2}, E_2 = \sqrt{\frac{1}{N} \sum_{i=1}^N (\theta_{2di} - \theta_{2ai})^2}$$

$$E_3 = \sqrt{\frac{1}{N} \sum_{i=1}^N (\theta_{3di} - \theta_{3ai})^2} \quad (33)$$

where N is the number of considered samples. θ_{1di} , θ_{2di} , θ_{1ai} , and θ_{2ai} , θ_{3i} are the desired angles of the active joints and real angles of the active joints at time index i respectively.

The simulation results of three control schemes consisting of traditional SMC, the controller [20], and the proposed controller for a 3-DOF planar parallel robot are shown in Figs. 5-10. Fig. 5 and Fig. 6 respectively show the desired path and the actual path of the end-effector in the XY coordinate system and the end-effector's rotation angle.

In this paper, we mainly focus on improving convergence speed and tracking accuracy. Look at the zoomed-in parts of Figs. 5, 6, and 7 in the reaching phase, it is easily seen that the trajectory under the proposed controller quickly approaches the desired trajectory. It has the fastest convergence among all of the three control methods.

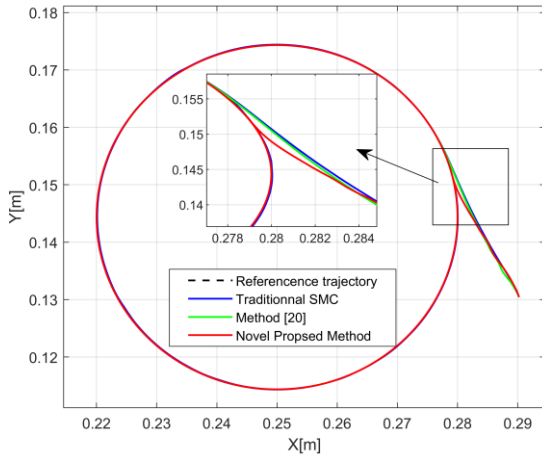


Figure 5. The desired path and actual path of the end-effector in the XY-coordinate system under three different controllers.

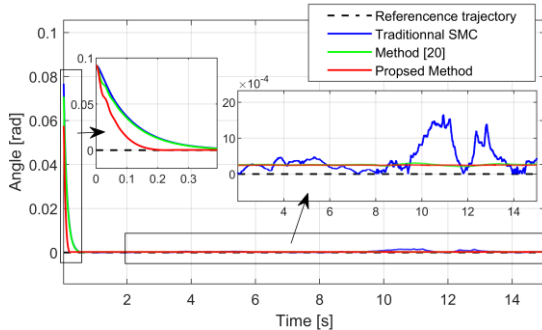


Figure 6. The desired path and actual path of the rotary angle of the end-effector under three different controllers.

In terms of tracking accuracy, the tracking simulation results from Figs. 5-7, and Table III shows that the proposed controller has the smallest control errors. It has better tracking accuracy than the method [20] (from 10^{-5} to 10^{-6} as shown in Table III).

TABLE III. THE ROOT MEAN SQUARE OF CONTROL ERRORS AT ACTIVE JOINTS OF THREE CONTROLLERS

| Control Methods | E_1 | E_2 | E_3 |
|-----------------|------------------------|------------------------|------------------------|
| SMC | 3.043×10^{-4} | 3.634×10^{-4} | 3.269×10^{-4} |
| Method [20] | 1.624×10^{-5} | 1.274×10^{-5} | 0.769×10^{-5} |
| Proposed Method | 1.181×10^{-6} | 0.927×10^{-6} | 0.500×10^{-6} |

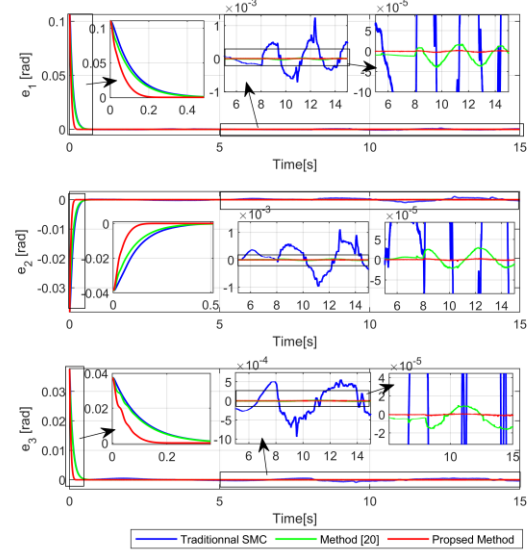


Figure 7. The control errors of joints under three control methods.

The control input signals of the three controllers are shown in Fig. 8. Both method [20] and the proposed controller have impressively reduced chattering behavior in their control signals. Because these controllers are applied RBFNN to reduce the effects of uncertainties and external disturbances. While the conventional SMC still exists serious chattering phenomena in its control signals because of the large sliding gain that is used to combat the effects of uncertain terms.

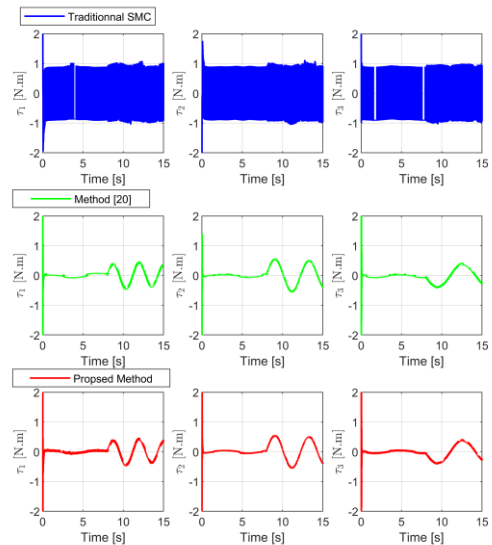


Figure 8. The control input signals of three control methods.

Fig. 9 shows the estimated values of the whole uncertainties and external disturbances under the controller [20] and the proposed controller.

Fig. 10 illustrates the adaptive values of sliding gain under the controller [20] and the proposed controller. By using an adaptive technique integrated into the reaching control law, the need for the upper bound values has been removed.

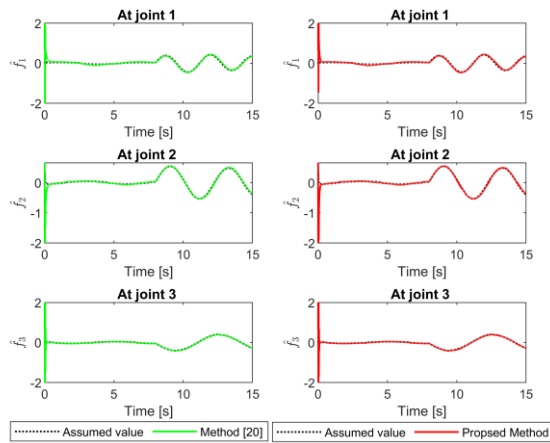


Figure 9. The estimated values of the whole uncertainties and controller [20] and the proposed controller.

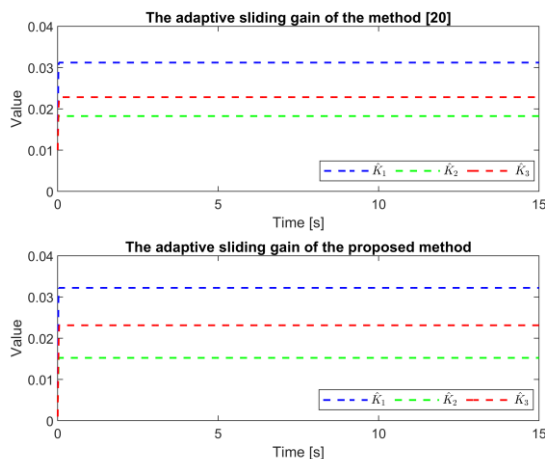


Figure 10. The adaptive values of sliding gain under controller [20] and proposed controller.

V. CONCLUSION

In this paper, we developed a novel ANSMC algorithm for 3-DOF parallel robotic manipulators which has a complicated dynamic model, including modeling uncertainties, frictional uncertainties, and external disturbances. The paper focuses on dealing with several limitations of conventional SMC, PID-SMC, and ISMC for 3-DOF robot manipulators at the same time. The paper has addressed three main points: improving the control accuracy, reducing chattering phenomena, and the convergence rate of the system states. To obtain the control objective, the proposed control method has been designed from the advantages of main control techniques, including ISMC, RBFNN, and the adaptive technique. Consequently, the proposed control system provides a higher tracking

accuracy and faster convergence rate than the classic SMC and method [20]. The chattering is significantly diminished in control signals and the requirement of upper boundary value for sliding gain is also eliminated by using the adaptive technique. A 3-DOF planar parallel manipulator has been designed by SolidWorks, then it has been embedded in MATLAB/Simulink environment in verifying the effectiveness of the proposed control system.

From the performance comparison, it could be concluded that the control performance of the proposed controller including tracking accuracy and fast convergence has been significantly enhanced compared to traditional SMC and controller [20]. The control proposal is high efficiency in the tracking control problems for 3-DOF planar parallel manipulators.

CONFLICT OF INTEREST

The authors declare no conflict of interest.

AUTHOR CONTRIBUTIONS

Conceptualization, methodology, validation, writing—original draft preparation, and writing—review and editing, T.N.T.; software, visualization, and resources, A.T.V.; supervision, funding acquisition, and project administration, H.-J.K.; formal analysis, and data curation, T.N.T., and H.-J.K. All authors have read and agreed to the published version of the manuscript.

FUNDING

This work was supported by Basic Science Research Program through the National Research Foundation of Korea (NRF) funded by the Ministry of Education (NRF-2019R1D1A3A03103528).

REFERENCES

- [1] K. D. Young and Ü. Özgüner, *Variable Structure Systems, Sliding Mode and Nonlinear Control*, vol. 247. Springer, 1999.
- [2] C. Edwards and S. Spurgeon, *Sliding Mode Control: Theory and Applications*. Crc Press, 1998.
- [3] T. N. Truong, A. T. Vo, H. J. Kang, and M. Van, “A novel active fault-tolerant tracking control for robot manipulators with finite-time stability,” *Sensors*, vol. 21, no. 23, December 2021.
- [4] C. Edwards, E. F. Colet, L. Fridman, E. F. Colet, and L. M. Fridman, *Advances in Variable Structure and Sliding Mode Control*, vol. 334. Springer, 2006.
- [5] A. T. Vo, T. N. Truong, and H. J. Kang, “A novel tracking control algorithm with finite-time disturbance observer for a class of second-order nonlinear systems and its applications,” *IEEE Access*, vol. 9, pp. 31373–31389, February 2021.
- [6] T. N. Truong, H. J. Kang, and A. T. Vo, “An active disturbance rejection control method for robot manipulators,” in *Proc. Int. Conf. on Intelligent Computing*, 2020, pp. 190–201.
- [7] A. T. Vo, T. N. Truong, H. J. Kang, and T. D. Le, “An advanced terminal sliding mode controller for robot manipulators in position tracking problem,” in *Proc. Int. Conf. on Intelligent Computing*, 2022, pp. 518–528.
- [8] T. N. Truong, A. T. Vo, H. J. Kang, and T. D. Le, “An observer-based fixed time sliding mode controller for a class of second-order nonlinear systems and its application to robot manipulators,” in *Proc. Int. Conf. on Intelligent Computing*, 2022, pp. 529–543.
- [9] I. Eker, “Sliding mode control with PID sliding surface and experimental application to an electromechanical plant,” *ISA Trans.*, vol. 45, no. 1, pp. 109–118, January 2006.

- [10] Y. J. Choi and M. C. Lee, "PID sliding mode control for steering of lateral moving strip in hot strip rolling," *Int. J. Control. Autom. Syst.*, vol. 7, no. 3, pp. 399–407, May 2009.
- [11] Y. Pan, C. Yang, L. Pan, and H. Yu, "Integral sliding mode control: performance, modification, and improvement," *IEEE Trans. Ind. Informatics*, vol. 14, no. 7, pp. 3087–3096, October 2018.
- [12] Y. Niu, D. W. C. Ho, and J. Lam, "Robust integral sliding mode control for uncertain stochastic systems with time-varying delay," *Automatica*, vol. 41, no. 5, pp. 873–880, May 2005.
- [13] T. N. Truong, A. T. Vo, H. J. Kang, and T. D. Le, "A neural terminal sliding mode control for tracking control of robotic manipulators in uncertain dynamical environments," in *Proc. Int. Conf. on Intelligent Computing*, 2021, pp. 207–221.
- [14] T. N. Truong, A. T. Vo, and H. J. Kang, "Implementation of an adaptive neural terminal sliding mode for tracking control of magnetic levitation systems," *IEEE Access*, vol. 8, pp. 206931–206941, November 2020.
- [15] A. T. Vo and H. J. Kang, "Neural integral non-singular fast terminal synchronous sliding mode control for uncertain 3-DOF parallel robotic manipulators," *IEEE Access*, vol. 8, pp. 65383–65394, April 2020.
- [16] Q. D. Le, H. J. Kang, and T. D. Le, "An adaptive position synchronization controller using orthogonal neural network for 3-DOF planar parallel manipulators," in *Proc. Int. Conf. on Intelligent Computing*, 2017, pp. 3–14.
- [17] Q. V. Doan, T. D. Le, Q. D. Le, and H. J. Kang, "A neural network-based synchronized computed torque controller for three degree-of-freedom planar parallel manipulators with uncertainties compensation," *Int. J. Adv. Robot. Syst.*, vol. 15, no. 2, p. 1729881418767307, 2018.
- [18] T. N. Truong, A. T. Vo, and H. J. Kang, "An adaptive terminal sliding mode control scheme via neural network approach for path-following control of uncertain nonlinear systems," *Int. J. Control. Autom. Syst.*, vol. 20, no. 6, pp. 2081–2096, June 2022.
- [19] *Jinkun Liu*, "Radial Basis Function (RBF) neural network control for mechanical systems: Design, analysis and Matlab simulation," Springer, 2013.
- [20] T. N. Truong, H. J. Kang, and T. D. Le, "Adaptive neural sliding mode control for 3-dof planar parallel manipulators," in *Proc. of the 2019 3rd Int. Symposium on Computer Science and Intelligent Control*, 2019, pp. 1–6.
- [21] T. N. Truong, A. T. Vo, and H. J. Kang, "A backstepping global fast terminal sliding mode control for trajectory tracking control of industrial robotic manipulators," *IEEE Access*, vol. 9, pp. 31921–31931, February 2021.
- [22] V. I. Utkin, *Sliding Modes in Control and Optimization*, Springer Science & Business Media, 2013.

Copyright © 2023 by the authors. This is an open access article distributed under the Creative Commons Attribution License (CC BY-NC-ND 4.0), which permits use, distribution and reproduction in any medium, provided that the article is properly cited, the use is non-commercial and no modifications or adaptations are made.



mechatronics.

Thanh Nguyen Truong received a Bachelor of Science diploma with a major in electrical engineering from University of Science and Technology, Danang, Vietnam, in 2018. His current research project is at the University of Ulsan, Ulsan, Korea, where he is pursuing a Doctor of Philosophy degree in electrical engineering. A major focus of his research is on robotic manipulators, sliding mode control and its applications, and advanced control theory for



interested in intelligent control, sliding mode control and its applications, and fault-tolerant control. More than 25 of his papers have been published in journals and international conferences.

Anh Tuan Vo graduated from University of Science and Technology in 2008 with a Bachelor of Science degree in electrical engineering, and he earned his Master of Science degree in automation from The University of Danang, Danang, Vietnam, in 2013. He graduated from the Graduate School of the University of Ulsan, Ulsan, South Korea, in 2021 with a Doctor of Philosophy degree in electrical engineering. Currently, he is working as a postdoctoral fellow at University of Ulsan, Korea. He is particularly



robot fault diagnosis, and mechanisms analysis, his current research interests encompass robot calibration, robot calibration, haptics, and mechanism analysis.

Hee-Jun Kang earned a Bachelor of Science degree in mechanical engineering from Seoul National University, South Korea, in 1985, and Master of Science and Doctor of Philosophy degrees in mechanical engineering from The University of Texas at Austin, USA, in 1988 and 1991, respectively. He joined the University of Ulsan in 1992 and is currently a Professor of Electrical Engineering. In addition to sensor-based robotics, haptics,